ACS APPLIED MATERIALS & INTERFACES

Research Article

www.acsami.org

Nanometer Smooth, Macroscopic Spherical Cellulose Probes for Contact Adhesion Measurements

Christopher Carrick,*[,†,‡] Samuel A. Pendergraph,[†,‡] and Lars Wågberg*[,†,§]

[†]KTH Royal Institute of Technology, School of Chemical Science and Engineering, Department of Fibre and Polymer Technology, SE-100 44 Stockholm, Sweden

[§]KTH Royal Institute of Technology, School of Chemical Science and Engineering, Wallenberg Wood Science Centre, WWSC, SE-100 44 Stockholm, Sweden

Supporting Information

ABSTRACT: Cellulose spheres were prepared by dissolving cellulose fibers and subsequently solidifying the solution in a nonsolvent. Three different solution concentrations were tested and several nonsolvents were evaluated for their effect on the formation of spheres. Conditions were highlighted to create cellulose spheres with a diameter of ∼1 mm and a root-mean-square surface roughness of ∼1 nm. These solid spheres were shown to be easily chemically modified without changing the mechanical properties significantly. Contact adhesion measurements were then implemented with these spheres against a poly(dimethylsiloxane) (PDMS) elastomer in order to quantify the adhesion. Using Johnson−Kendall−Roberts (JKR) theory, we quantified the adhesion for unmodified cellulose and hydrophobic cellulose spheres. We highlight the ability of these spheres to report more accurate adhesion information, compared to spin-coated thin films. The application of these new cellulose probes also opens up new possibilities for direct, accurate measurement of adhesion between cellulose and other materials instead of using uncertain surface energy determinations to calculate the theoretical work of adhesion between cellulose and different solid materials.

KEYWORDS: *cellulose, adhesion, surface roughness, contact adhesion, spheres, chemical modification*

INTRODUCTION

Cellulose has been an extensively studied material over several decades, because of the natural abundance and the excellent mechanical properties of fibers that consist primarily of crystalline cellulose.[1−4] Advances in the production of various types of cellulose and cellulose derivatives have enabled a plethora of applications to be realized, including structural composites,[4,5] energy-related devices,[6,7] and food modifiers.[8] Considerable research has also been focused on the stability of cellulosic products in solution.[8] New strategies have been utilized to form stable nanocellulose dispersions in order to introduce these robust materials into composites or to control the fiber orientation upon drying.[9,10] Through chemical modification of the accessible cellulose surface molecules, stable and more mechanically robust interfaces have been produced. Typically, modification of fibers, either through covalent bonding or through electrostatic attachment of polyelectrolytes or nanoparticles, has been shown to be effective to suppress the aggregation of cellulosic materials.[1,5,11−16] One successful example has been the chemical modification of cellulose to enable their incorporation into synthetic polymers for fiber-reinforced composites.[4,5] However, it has been challenging to quantify the adhesion between the cellulose fibers and matrix polymers, since the measurement of molecular interactions requires smooth and homogeneous surfaces, as well as specific bulk material properties (i.e., modulus). Furthermore, since the surface roughness plays a vital role, there is no general strategy to understand the normal adhesion at length scales larger than what is allowed in atomic force microscopy (AFM) colloidal probe testing,[17,18] using thin cellulose model surfaces.[19−21] Model films are commonly attached to silicon wafers, using cationically charged anchoring polymers, and thin films of cellulose have been the primary method to quantitatively measure interfacial behavior of cellulose. Adhesion of cellulose interfaces have been studied through AFM probe measurements and surface force apparatus (SFA) measurements, which have provided quantification of these interfaces.[17,18,22,23] While these techniques have provided useful information on the effect of the modification of cellulose, it must be stressed that the adhesive strengths evaluated in this manner were measured in a highly confined thin-film regime. Wågberg and co-workers have demonstrated cellulose adhesion measurements with a macroscopic contact adhesion apparatus in order to elucidate more-comprehensive data, such as the advancing and receding surface energies.[19−21] While these measurements provided the first platform for imaging and

Received: August 22, 2014
Accepted: November 10, 2014
Published: November 10, 2014

quantifying the adhesion, the surface interactions were still predicated on the use of thin films with anchoring polymers. Other researchers have documented significant discrepancies that can arise in the adhesion energies from using thin films compared to bulk materials.[24−26] In order to elucidate the true adhesion interactions of cellulosic interfaces, smooth bulk materials are needed.

In this report, we describe a procedure to form bulk cellulose spheres with minimal roughness at the surface. Specifically, we highlight the conditions that enable spheres with a dry diameter up to 1 mm and a root-mean-square (rms) roughness of 1 nm to be formed. To our knowledge, cellulose interfaces with rms values of 1 nm have only been approached by spin-coating thin films or by implementing monolayers of crystalline nanocellulose.[27] However, the cellulose spheres presented in this study were then utilized in macroscopic contact adhesion testing to determine the work of adhesion as the interfaces are brought into contact and separated while using the bulk mechanical properties of both cellulose and matrix material. We also show that it is possible to quantify the change in the work of adhesion through simple chemical modification of the cellulose spheres to a lower surface energy material, and we also discuss the potential implications of these new abilities.[4]

EXPERIMENTAL SECTION

Materials. Dissolving pulp (Domsjö Dissolving Plus) was provided by Aditya Birla, Domsjö Fabriker AB, Sweden. These fibers contained 93% cellulose with a surface charge of 29 μmol charges/g fibers with a degree of polymerization of ∼780 (provided by the manufacturer). *N*,*N*-dimethylacetamide (DMAc) (>99.5%, GC grade), lithium chloride (LiCl), tetrahydrofuran (THF) (99.9%, anhydrous), ethylene glycol (99.8%, anhydrous), methanol (99.93%, bioreagent grade), acetone (>99.9%, HPLC grade), heptane (99%, anhydrous), silicone oil, methylene iodide (99%), and undecenoyl chloride (97%) were purchased from Sigma−Aldrich and used as received. Triethylamine (TEA) (99+%), silicone oil, and dichloromethane (DCM) (99.8%, HPLC grade) were purchased from VWR and used as received. Sylgard 184 prepolymer and curing agent was purchased from Dow Corning.

Preparation of Cellulose Solution. The cellulose fibers were dissolved in a mixture of 5 wt % LiCl in DMAc, according to a previously described protocol.[28] Before adding cellulose to the solvent mixture, which is highly hygroscopic, the solvent was heated to 105 °C for 30 min to remove traces of water. If water is still present in the solvent, it impairs the dissolution of cellulose[29] and promotes the formation of molecular aggregates.[30] Different amounts of oven-dried pulp were then rewetted and swollen in the LiCl−DMAc mixture and subsequently added in different amounts to reach different cellulose concentrations, using a final total volume of 100 mL. The solution was then reheated to ∼80 °C to further facilitate the dissolution of cellulose. The cellulose solution was then centrifuged at 14 000 rpm for 15 min and filtered through a 0.45-μm polytetrafluoroethylene (PTFE) syringe filter to remove traces of nondissolved cellulose, if present.

Preparation of Cellulose Spheres. Cellulose spheres were based on a solution solidification method.[31] Dissolved cellulose in LiCl−DMAc solution (3 mL) were added dropwise from a height of ∼1 cm into 30 mL of a bath of a nonsolvent, Milli-Q water, ethanol, acetone, THF, or methanol, where the cellulose solidified as spherical drops. The prepared cellulose spheres were then left to equilibrate first for 24 h, resting in the nonsolvent. Next, for 1 week, the spheres were exchanged one time per day with fresh nonsolvent to ensure a proper removal of the cellulose solvent. Finally, the probes were dried at room temperature for 48 h. Spheres dried from methanol at 5 °C were dried for 7 days. The sphere diameter was determined using optical microscopy to obtain images of the spheres and ImageJ software to quantify the diameter. The sphere diameter was determined over an average of 12 different spheres.

Acylation. Acylation of the cellulosic material was performed by weighing the solidified, amorphous cellulose spheres to be modified. After measuring this weight (typically ∼0.01 g), the number of moles of hydroxyl groups was calculated by dividing the measured mass by the molecular weight of the glucose repeat unit in cellulose. A 10-fold molar excess of TEA (compared to number of glucose repeat units) was added to 10 mL of THF in a glass vial. The vial was subsequently capped with a rubber septum and then placed in an ice bath for 5 min to cool the solution down. Next, a 10-fold molar excess of undecenoyl chloride (equimolar to TEA) was added dropwise via syringe. The reaction mixture was subsequently heated to room temperature and reacted overnight (∼15 h). After this reaction, the cellulose spheres were washed thoroughly 3 times with DCM. The spheres were placed in a vial with DCM and sonicated with a sonication bath for 5 min; the wash was subsequently discarded and repeated three more times to ensure the removal of unreacted reagents and TEA salts from the cellulose. The remaining cellulose spheres were allowed to dry at room temperature for 48 h before subsequent analysis or adhesion testing.

INSTRUMENTATION

Characterization of the Cellulosic Sphere Morphology, Shape, and Surface Profile. The cellulose sphere's dimensions and morphology were characterized from images collected with a field-emission scanning electron microscopy (FE-SEM) system (Hitachi, Model S-4800) operating at high vacuum.

The topography and surface roughness of the dried cellulose spheres were characterized using an atomic force microscopy (AFM) system (Multimode Nanoscope IIIa, Bruker Corp., USA) operating in Scanasyst mode with a cantilever that had a spring constant of 5 N m^{-1} and a radius of ∼8 nm (Bruker Corp., USA).

X-ray diffraction (XRD) was conducted with a PANalytical XPert Pro powder diffractometer with Cu Kα radiation (λ = 0.1541 nm) at 25 °C. The scanning angle (2θ) was measured from 5° to 70° at a step size of 0.0172°.

Tensile Bulk Mechanical Properties of Cellulose Film. The mechanical properties of cellulose films were prepared by pouring 1.5 wt % cellulose solution into a large glass Petri dish. Next, the solution was solidified by allowing the film to absorb water from the ambient environment until a solid film was formed at room temperature. The films were washed continuously with ethanol for 48 h. The films were then allowed to dry at room temperature for 7 days. Cellulose films were cut into dogbone-shaped test pieces of 16 mm in length and 4 mm in width. Samples that were acylated were functionalized in the same manner as the spheres. The samples were then conditioned at 23 °C and 50% relative humidity for 24 h prior to tensile testing. PDMS dogbone-cut films were analyzed using an Instron 5566 with a 500-N load cell. Three 16-mm dogbone samples of the different cellulosic materials were strained at 1.6 mm/min.

Contact Adhesion Measurement. A transparent cellulose sphere with a typical radius of 0.9 mm carefully attached with a cyanoacrylate glue to a silicon wafer. In our contact adhesion setup,[21] the cellulose probe was moved toward the opposing flat, 4-mm-thick PDMS film at a rate of 10 μm min^{-1} to a trigger value of 1 g (9.8 mN). After this critical load was reached the probe was retracted from the PDMS surface at a rate of 10 μm min^{-1} until separation of the surfaces occurred. The data acquisition rate for both the loading measurements and contact radius images was 120 data points min^{-1}. The cellulose probe and the PDMS surface had been allowed to

equilibrate before the experiment in a controlled environment of 23 °C and 50% relative humidity for at least 24 h.

Contact Angle Measurements of Cellulose Model Surfaces. Static contact angle measurements were performed with Milli-Q purified water, methylene iodide, and ethylene glycol, using a KSV CAM 200 contact angle monometer (KSV Instruments, Helsinki, Finland) for three different cellulose model surfaces and for three different acylated cellulose model surfaces. The model surfaces were prepared similar to standard procedures,[32] where a drop from the same dissolved cellulose solution, as used for the sphere preparation, was deposited on a silica surface and then spin-coated using a KW-4A spin-coater (Chemat Technology, CA, USA) operating at initial speed of 1500 rpm for 15 s, and then 3500 rpm for another 30 s, and were dried at room temperature. Prior to the contact angle measurements, the model surfaces were conditioned at 23 °C and 50% relative humidity for 24 h. The contact angles reported in this study were measured 20 s after the drop was applied on the model surfaces to get stable static contact angles, since the initial contact angles were not stable, because of liquid penetration into the model films. The surface energies were calculated according to eq 1,[33,34] where the surface energy is separated into a dispersive energy component (γ^d) and polar energies consisting of acid (γ^+) and base (γ^-) contributions:

$$\frac{(1+\cos\theta)\gamma_l}{2} = \sqrt{\gamma_s^d\gamma_l^d} + \sqrt{\gamma_s^-\gamma_l^+} + \sqrt{\gamma_s^+\gamma_l^-} \quad (1)$$

The method requires the use of three different solvents, since the equation consists of three unknown variables. Here, we used water, methylene iodide, and ethylene glycol with known surface energy components taken from the literature.[35] The calculated values of the surface energies of the cellulose and the acylated cellulose surface can be found in the Supporting Information.

RESULTS

Preparation of Smooth Cellulose Spheres and Films. Dissolution of the pulp in DMAc–LiCl enabled the formation of the materials into films and spheres for characterization of the bulk properties. The dissolved solution was taken and then solidified in various nonsolvents, shown in Figure 1. In Figure 1c, the cellulose spheres are shown to be stable in various solvents. This chemical stability allowed for chemical modifications without dissolving the sphere or inducing defects on the surface.

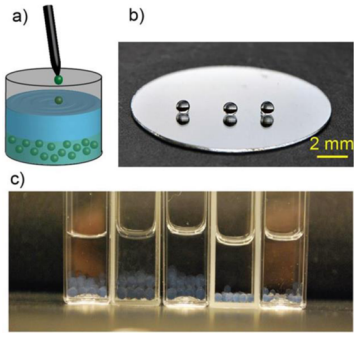

Figure 1. (a) Schematic illustration of the cellulose sphere preparation method where a dissolved cellulose droplet was deposited dropwise into ethanol and the cellulose subsequently solidified into a sphere. (b) Photograph of three dried cellulose spheres, resting on a mirror, solidified from a 1.5 wt % cellulose solution in ethanol. The cellulose sphere's insolubility in various solvents is represented in panel (c), where the cellulose spheres had been solvent-exchanged with (from the left to right) water, acetone, ethanol, heptane, and silicone oil.

Initially, before the dissolution of the cellulose-rich fibers, the fibers were partially crystalline, containing peaks at 17° and 23°, which corresponded to the [101] and [002] crystal planes (see Figure S1 in the Supporting Information). After dissolution of the cellulose and the subsequent solidification, it was obvious that the crystallinity of the sample was decreased since a broad peak appeared at 20°, which corresponded to an amorphous cellulose polymer.[36] Films of the cellulose were then uniaxially strained to evaluate the modulus. Bulk films of cellulose and acylated cellulose had a tensile modulus of 3.8 ± 0.2 and 3.1 ± 0.6 GPa, respectively, using a displacement rate of 1.6 mm min^{-1}.

In order to optimize the conditions for forming spheres, three concentrations of the cellulose in the DMAc–LiCl solvent were tested: 1.0, 1.5, and 2.0 wt % (corresponding viscosities were 70, 300, and 1050 mPa s, respectively), based on previous procedures for forming hollow spheres.[31,37] When using 1 wt % cellulose concentration, large wrinkles on the sphere surface were created upon drying (see Figure S2 in the Supporting Information). Increasing the cellulose concentration to 2 wt % created elliptically shaped particles (see Figure S2 in the Supporting Information). By implementing a 1.5 wt % cellulose concentration, the wrinkles were suppressed and a spherical geometry was obtained, as shown in Figure 2a. The prepared spheres were then functionalized by acylating the cellulose spheres to change the surface energy (see Figure 2b).

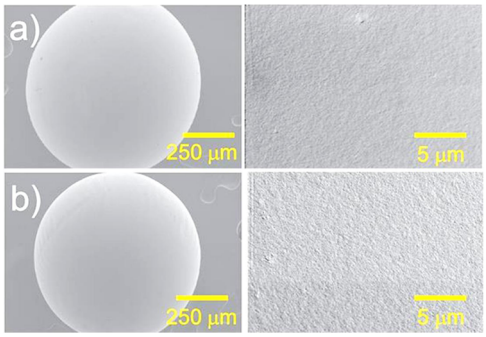

Figure 2. Cellulose spheres solidified from a 1.5 wt % cellulose solution in ethanol and dried in room temperature where panels (a) and (b) represent electron micrographs of the top view morphology of the cellulose sphere and the acylated sphere, respectively. The left and right micrographs represent the entire sphere and the surface morphology of the respective cellulose sphere.

Surface Roughness. The surface roughness of the solidified cellulose spheres were analyzed using AFM where the rms roughness of the acylated and the nonacylated cellulose spheres was measured to be 1.0 ± 0.2 nm and 6.3 ± 0.3 nm, respectively (see Figures 3a and 3b). If the nonacylated spheres were submerged in THF and dried a second time, following the same procedure without the esterification, the surface rms roughness value was further decreased to 2.0 ± 0.2 nm (Figure 3c). This roughness was comparable to previous reported values on smooth cellulose thin films used for adhesion measurements.[19]

Surface Energies Measured by Contact Angle Measurements. Experimental determination of the surface energies

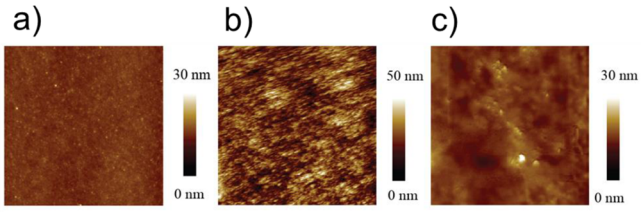

Figure 3. Atomic force height measurement (3 μm × 3 μm) of (a) the cellulose surface functionalized with acylation, which had been swollen and redried from THF, (b) cellulose surface dried once from ethanol, and (c) cellulose surface swollen and redried from THF.

of cellulose and acylated cellulose model surfaces was conducted by contact angle measurements using water, ethylene glycol, and methylene iodide solutions and calculated using eq 1. A full table of the dispersive and polar contributions to the surface energy can be seen in Table S1 in the Supporting Information. Acylation of the cellulose resulted in a more hydrophobic surface, as shown in Figure S4 in the Supporting Information. The contact angle measurements showed that the cellulose probes were chemically modified since the total surface energy decreased from 64.3 mJ/m^2 to 40.3 mJ/m^2. The polar contribution of the surface energy of the acylated cellulose decreased substantially as expected, where the dispersive energies remained similar to the cellulose probes, which also was expected. The work of adhesion from contact angle measurements (W_{12}) (Table 1) was calculated from eq 2:

$$W_{12} = 2\sqrt{\gamma_1^d \gamma_2^d} + 2\left(\sqrt{\gamma_1^+ \gamma_2^-} + \sqrt{\gamma_2^+ \gamma_1^-}\right) \quad (2)$$

where γ_1 and γ_2 are the surface energies of PDMS and cellulose, respectively.

Table 1. Work of Adhesion between Cellulose/Acylated Cellulose and PDMS from Contact Angle Measurements (W_{12}), Determined Using Equation 2[a]

	Value	
parameter	cellulose	acylated
W_{12}^{tot} (mJm^{-2})	65	60
W_{12}^{d} (mJm^{-2})	62	59
W_{load} (mJm^{-2})	41 ± 5	40 ± 4
W_{unload} (mJm^{-2})	104 ± 5	142 ± 13
G_c^{b} (mJ/m^{-2})	107 ± 10	143 ± 12

[a]The W parameter from the loading and unloading experiments were determined by the Johnson–Kendall–Roberts (JKR) model calculations (eq 3) using the contact macroscopic adhesion measurement. [b]G_c represents the work of adhesion at the maximum separation force (eq 6).

The values for the PDMS were taken from literature values.[38] The surface energy values of cellulose were experimentally determined from contact angles using water, ethylene glycol, and methylene iodide.

Macroscopic Contact Adhesion Testing. Johnson–Kendall–Roberts (JKR) measurements of cellulose surfaces have previously been performed using thin films (10–40 nm) of cellulose model surfaces.[19,20,32] Thin films have been utilized due to the low surface roughness that can be obtained. In the present work, a macroscopic cellulose sphere was used in contact adhesion testing and in order to determine the mechanical properties of these cellulose materials.

The cube of the contact radius, a^3, and the applied load (F) were related to the work of adhesion (W) between the sphere and the flat surface in contact, according to JKR theory (eq 3).

$$a^3 = \frac{R}{K}\left[F + 3\pi WR + \sqrt{6\pi WRF + (3\pi WR)^2}\right] \quad (3)$$

where K is the elastic constant of the system and R is the radius of curvature for the two surfaces, which can be described as the following:

$$\frac{1}{R} = \frac{1}{R_1} + \frac{1}{R_2} \quad (4)$$

The elastic modulus (E) can be related to K by eq 5:

$$\frac{1}{K} = \frac{3}{4}\left(\frac{(1-\nu_1^2)}{E_1} + \frac{(1-\nu_2^2)}{E_2}\right) \quad (5)$$

where ν_1 and ν_2 are the Poisson's ratio for the two materials in contact and E_1 and E_2 are the elastic moduli of the respective materials. The elastic constant of the system was found to be 4.00 ± 0.06 and 4.10 ± 0.10 MPa for cellulose and acylated cellulose pressed against a PDMS surface, respectively, for both the loading and unloading sections of the curve.

The adhesion energy at the critical pull-off force (G_c) was calculated from eq 6:

$$F_s = \frac{3}{2}\pi R G_c \quad (6)$$

where F_s is the force when the surfaces spontaneously separate.

The G_c values for the cellulose and acylated samples from eq 6 were 107 ± 10 and 143 ± 12 mJ/m^2, respectively.

The results from the JKR measurements are shown in Figure 4 for the cellulose and acylated cellulose probes, respectively. The work of adhesion for the loading and unloading was calculated according to eq 3 and is compiled in Table 1.

DISCUSSION

Properties of Cellulose Spheres. The preparation conditions were investigated to prepare spherical cellulose probes with low surface roughness. First, the effect of the nonsolvent solidifying the cellulose solution was evaluated. Water was tested first as the nonsolvent, with a dripping height of 1 cm above the nonsolvent surface. The cellulose droplets spread on surface rather than penetrating through the surface. When the dripping height was increased to ∼10 cm above the surface, the droplet penetrated through the water surface. However, this higher dripping height influenced the shape and surface profile of the cellulose spheres. Water was not an acceptable nonsolvent, because of the inability of water to form spheres without creating significant defects on the surface. Therefore, the surface tension was reduced in order to allow the droplets to solidify without being affected by the impact of higher dripping heights.

By incorporating a lower surface tension fluid, acetone (1:1 volumetric ratio with water),[39] a dripping height of 1 cm was sufficient to allow the drop to penetrate the surface and to induce a rapid solidification. Introducing acetone into the mixture resulted in buckles on the cellulose surface upon drying. Using pure acetone also created defects, since the cellulose droplets were fairly miscible with acetone and subsequently solidified into spherical shaped particles with surface defects. Methanol was subsequently tested, since it possessed a similar surface tension to acetone; however, it has a

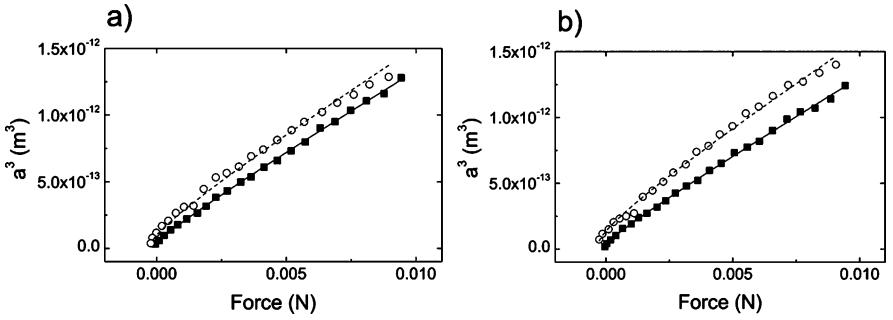

Figure 4. JKR fitting of the results from the adhesion experiments using (a) nonmodified cellulose spheres and (b) acylated cellulose spheres by forcing the probe in contact with a flat PDMS surface, where the loading is represented by solid squares and the unloading is represented by unfilled circles. The lines are fitted to the JKR equation (eq 3). The experiment was performed at 23 °C and 50% RH at a displacement rate of 10 μm/min where the elastic constant (K) of the systems was calculated to be 4.00 ± 0.06 and 4.10 ± 0.10 MPa for cellulose and acylated cellulose, respectively.

Table 2. Cellulose Probes and Films Used for Adhesion Measurements[a]

cellulosic interface	thickness/ diameter	average roughness	W_{load} (mJ/m^2)	W_{unload} (mJ/m^2)	G_c (mJ/m^2)	ref
nanocellulose layer by layer prepared film versus PDMS sphere	4−9 nm	0−1 nm	49.5	NP	201	21
a solidified cellulose film from a dissolved cellulose in NMMO solution versus PDMS	30 nm	3.9 nm	47	NP	389	20
dissolved cellulose in DMAc/LiCl solidified on a silica wafer versus PDMS	44 nm	1.9 nm	46	NP	472	20
cellulose nanocrystal film versus PDMS	120 nm	2.3 nm	45	NP	289	20
spin-coated nanocellulose fibrils on a silica wafer versus nanocellulose fibrils on a PDMS cap	11 nm	1.7 nm	47	65	59	19
cellulose microsphere versus a cellulose sphere modified with polycaprolactone	10−15 μm	32 nm	NA	NA	422[b]	17
cellulose spheres versus PDMS	920 μm	2 nm	41 ± 5	104 ± 5	107 ± 10	present work
acylated cellulose sphere versus PDMS	930 μm	1 nm	40 ± 4	142 ± 13	143 ± 12	present work

[a]The table demonstrates where the adhesion has been calculated using two methods: JKR and AFM. Furthermore, the table demonstrates where it has not been possible (NP) to calculate the adhesion using the JKR theory, because of, e.g., large hysteresis and large deviations from the JKR figure (a^3 versus force). [b]G_c was recalculated from their data, in this example cellulose functionalized with poly(caprolactone) was tested. The W_{unload} value for previous studies was not possible (NP), because of inconsistencies in the elastic constant (K). The parameters W_{load} and W_{unload} are not applicable (NA), since there was no controlled way of determining the contact area.

different polarity. Similar to acetone, methanol produced defects on the surface of the spheres. However, one modification to mitigate the roughness with methanol was to dry the spheres at 5 °C. Although the drying time was considerably longer (5 days longer), there was a reduction in the roughness (see Figure S3 in the Supporting Information). Ethanol was the nonsolvent that produced the best results regarding particle shape and surface roughness when drying the spheres at room temperature, shown in Figure 2a. The average size of the spheres (12 spheres measured) was 0.90 ± 0.03 mm. Overall, reducing the surface tension by a factor of ∼3 enabled the materials to be solidified rapidly at a dripping height of 1 cm.[39]

When using ethanol as the nonsolvent, the cellulose solution could penetrate the surface effectively and form smooth spheres. The optimum concentration of dissolved cellulose solution was 1.5 wt % (Figure 2). When decreasing the cellulose concentration to 1 wt %, the spheres started to buckle upon drying (see Figure S2 in the Supporting Information). Using a 2 wt % cellulose solution created elliptical particles with a characteristic tail (see Figure S2 in the Supporting Information). This was presumably due to a higher viscosity of the cellulose (1095 mPa s, compared to 301 mPa s for the 1.5 wt % cellulose concentrations).[31] The concentration of the dissolved cellulose was important to allow the appropriate amount of time for the solution to solidify and minimize defects in the sphere formation.

There was a constraint on how much nonsolvent was required to form the smooth spheres. At a final concentration of 9 vol % of the dissolved cellulose solution relative to the total volume, a phase-separated layer of LiCl−DMAc appeared at the bottom of the beaker, where the spheres rested. The spheres remained solidified in this phase-separated layer for 24 h and were then subsequently solvent-exchanged. We believe this dwell time in the LiCl−DMAc separated layer slowed the solvent removal from the spheres and consequently reduced the defects that were introduced. When the final concentration of the cellulose solution was decreased (∼1 vol %), the solution became homogeneous in appearance. Conversely, the spheres solidified with roughness on the surface. Maintaining a layer of LiCl−DMAc at the bottom of the ethanol bath was critical in maintaining a low roughness surface.

In Figure 3, the rms roughness of the cellulose was 6 times higher, compared with that of the acylated cellulose sphere. It was unclear whether the difference was from the chemical functionalization of the cellulose or from the processing conditions themselves (i.e., reaction solvents). We elucidated this question by rewetting the dried unmodified cellulose spheres in pure THF without acylation, and this decreased the rms roughness from 6.3 ± 0.3 nm to 2.0 ± 0.2 nm. When spheres swollen with ethanol were directly solvent exchanged

from ethanol to THF and then dried, rather than redried and immersed in THF, the surface roughness did not change. When the spheres were dried from ethanol and then rewetted with ethanol, the surface roughness also did not change. Using THF as the nonsolvent was not possible, since the solvent did not solidify the cellulose fast enough. The cellulose droplets aggregated into nonspherical cellulose-shaped particles, similar to that observed when using acetone. It was unclear why the use of THF with dried spheres decreased the roughness. For consistency with the acylated probes, the unmodified cellulose was rewetted with THF and dried to keep the roughness minimal in the adhesion testing.

Adhesion Measurements Using the Johnson–Kendall–Roberts (JKR) Approach. As can be seen in Table 2, the large cellulose spheres had comparable roughness as cellulose thin films previously used for adhesion testing.[19,22,27] However, thin films (11 nm in thickness) of cellulose do not reflect the true bulk properties of cellulosic materials, because of the high degree of confinement on the supporting silicon wafer. Thicker cellulose samples have been used, such as spheres with diameters of 10−15 μm. AFM measurements were implemented to study the adhesion of these polymer-grafted cellulose spheres.[17] The spheres in the aforementioned study were relatively rough, having an rms value of 32 nm, which was an order of magnitude larger than our system, which had an rms value of 1−2 nm.[40] Another drawback was that the contact area was not measured when using AFM probe testing, because of the difficulties of imaging small contact areas associated with probe sizes of 10−15 μm. It was also inconclusive to whether the AFM probe evaluated the materials in the bulk material regime or in a confined testing geometry. In this work, the cellulose probes had an average diameter of 0.90 ± 0.03 mm, which was almost 2 orders of magnitude larger in diameter than existing probes.[40] However, we would like to emphasize that our technique is a complementary technique to that of AFM probe adhesion testing. For example, smoother colloidal probes (rms roughness of 5.9 nm over an area of 1 μm × 1 μm) and smooth cellulose model surfaces (the rms roughness over an area of 1 μm × 1 μm was 1.4 nm)[41] was used to determine the Hamaker constant of cellulose.

The increased probe size has enabled the observation of the contact area that previously has been unattained. Previous studies on soft adhesion have shown that, when the contact radius was greater than 10% of the film thickness (h) (i.e., $a/h > 0.1$), confinement effects from the substrate were observed.[24,42] In order to maintain a bulk elastomeric material while using the cellulose spheres produced from the new solidification technique, we controlled the elastomer thickness to keep this dimensionless ratio $a/h < 0.1$. The unmodified cellulose sphere had a maximum contact radius of 130 μm with an applied load of 9.8 mN. Therefore, we created a PDMS substrate with a thickness of ∼4 mm to allow variability in the contact radius of the acylated samples and remain outside a confinement region ($a/h \approx 0.0325$).[24,43] Bartlett and Crosby[43] recently published a study on the effects of the stiffness and contact area of the system in normal adhesion. At constant contact area and surface chemistry, the adhesion can be altered by modification of the stiffness of the system. The compressive stiffness in the loading section was 5640 ± 930 N/m and 6050 ± 400 N/m, for cellulose and the acylated cellulose spheres, respectively, which represented a 7% difference in the system stiffness between the two samples. The diameter of the spheres was 0.92 and 0.93 mm for the cellulose and the acylated cellulose, respectively. Although the rms roughness (∼1−2 nm) of the surface of the cellulosic spheres was low, we needed to ensure that the contact area was not compromised because of these small asperities. Therefore, we applied an approximation for the compliant PDMS elastomer to ensure that the material would conform to the roughness.[42,44−46]

The ratio of the G_c and the elastic modulus (E) gives an approximate adhesive length scale that determines the distance over which adhesive forces are significant, as shown in eq 7:[42]

$$\delta_c \approx \frac{G_c}{E} \tag{7}$$

In eq 5, there were two elastic moduli in the system; however, since the elastic modulus of cellulose was 3 orders of magnitude higher than typical values of Sylgard 184, the contribution from cellulose was neglected. Application of eq 5 to the fitted constant K and assuming $\nu_1 = 0.5$ for PDMS, resulted in a modulus of E = 2.25 MPa, which was consistent with previously reported values.[47,48] The G_c values for cellulose and acylated cellulose from eq 6 were 107 ± 10 and 143 ± 12 mJ/m^2, respectively, at a testing velocity of 10 μm/min. The length over which adhesion should occur was then calculated from eq 7, which was 46 and 63 nm for the cellulose and acylated cellulose, respectively. These adhesive lengths were over an order of magnitude higher than the rms roughness of the cellulose surface. This indicated that the roughness would not prevent molecular contact from being established on the cellulose surface. Therefore, we anticipated that any differences in the adhesion would arise primarily from the surface interactions and not from the increase in the total stiffness or increase in contact area.

The cellulose and acylated cellulose both have similar work of adhesion in the loading sections. Although their total surface energies were different from the static contact angle measurements, the dispersive component of the surface energies were similar. Previous work on the adhesion of PDMS has suggested that the dispersive component of the surface energy was the predominant factor in the loading work of adhesion for JKR studies, compared to contact angle measurements.[49] When the probes were retracted and subsequently detached, the unloading work of adhesion was 36% higher with the acylated cellulose opposed to the unmodified cellulose. There was larger hysteresis observed for the acylated cellulose probe. We suggest that this was caused by the interactions between the alkyl chains on the periphery of the cellulose sphere and the PDMS elastomer. Since PDMS is a low T_g polymer, this allowed the monolayers on the acylated cellulose to interact, even at small contact times.

These smooth cellulose spheres have enabled JKR measurements in the unloading section that previously have been unable to measure. In these previous studies of cellulosic interfaces, large hysteresis has been reported and the only data that could be obtained was the work of adhesion at the critical pull-off force (G_c) from eq 6 and the loading data from the JKR analysis. The unloading data in these previous studies could not be used in the JKR analysis, because of the inconsistent elastic constant between the loading and unloading sections of the adhesion test. In these examples, the G_c values were a factor of ∼2 higher than our measurements.[20,21] One reason for this discrepancy was the mechanical stiffness differences between the cellulosic interfaces. In these prior studies, there was a thin film of cellulose on a silicon wafer. The thin film was highly confined and conversely was influenced by the mechanical

properties of the silicon wafer. However, in our experiments, the cellulose probe was a true bulk material, thus possessing a lower effective stiffness than the previously used thin film examples. Several studies have been published recently addressing this confinement effect on the critical pull-off force in unstable crack propagation, noting that higher confinement with a rigid substrate resulted in higher adhesion forces.[24−26,42,43]

The work of adhesion calculated from the surface energies of the individual materials was also obtained through static contact angle measurements. Our calculated work of adhesion was not substantially different (8% between cellulose and acylated cellulose), which was not consistent with the difference obtained from contact adhesion testing (i.e., from the receding part of the measurements). Furthermore, the work calculated from the contact angles had an intermediate value between the loading and unloading work of adhesion. Another problem that has been observed with the contact angle testing was the influence of the supporting substrate. In previous work, the same film supported on two different substrates, reported two different work of adhesion values, which indicated the influence of underlying material.[19]

Our cellulosic spheres provided an interface that was smooth enough to test adhesion measurements, yet replicate the mechanical response of bulk cellulose. The use of cellulose directly circumvents the difficulties associated with thin films. Surface modification of these spheres was shown to be stable. Since the cellulose probes exhibit high stability in various solvents, this enabled chemical modifications to be performed without significantly compromising the mechanical integrity of the cellulose. Altering the surface of the PDMS probes have also been shown to be problematic, because of the low surface energy of silicones and hydrophobic recovery of the silicate layers needed for the hydroxyl groups.[50,51] We anticipate the presence of hydroxyl groups and the stability of these groups to be of great value not only to the cellulose community, but also for general adhesion studies, where fundamental polymeric adhesion problems are investigated.

CONCLUSIONS

We have described a new procedure to form bulk cellulose spheres by solidification of dissolved cellulose. By carefully controlling the solidifying nonsolvent, the dripping height, cellulose concentration of the solution, and final concentration of the nonsolvent/cellulose solution mixture, spheres with rms roughnesses of ∼1 nm (measured over an area of 3 μm × 3 μm) were obtained. These spheres were then demonstrated to undergo simple chemical functionalization without significantly altering the bulk mechanical properties. The work of adhesion from the loading data, using the JKR theory, was ∼40 mJ/m^2 for both the unmodified and the acylated cellulose probes, which was similar to previously reported values. The cellulose spheres enabled the evaluation of the unloading adhesion, which was not possible in prior experiments with rigidly supported thin films. We anticipate this method of adhesion testing to provide more-accurate adhesion information on interfacial behavior of cellulosic and paper products. Furthermore, we believe these probes can have a valuable impact on other adhesion science problems, because of the stability of the functional groups and the ease to functionalize the periphery of the sphere without compromising the mechanical properties of the probe.

ASSOCIATED CONTENT

Supporting Information

SEM images of dried samples in various processing conditions, XRD analysis of the cellulose spheres, contact angle photographs of the cellulose and modified surfaces, and a movie of the contact adhesion testing are shown in the Supporting Information. This material is available free of charge via the Internet at http://pubs.acs.org.

AUTHOR INFORMATION

Corresponding Author

*E-mail: wagberg@kth.se (L.W.).

Author Contributions

‡These authors contributed equally to the manuscript.

Notes

The authors declare no competing financial interest.

ACKNOWLEDGMENTS

C.C. and L.W. would like to thank Pulpaper Machinery AB and Wallenberg Wood Science Center for financial support. S.A.P. would like to thank the KAMI Research Foundation for financial support. The authors would like to thank BiMaC at KTH for financial support on the project. The authors would like to thank Dr. Michael D. Bartlett for invaluable discussions on the adhesion testing. The authors would like to thank Andrew Marais for assistance on the photographic images.

REFERENCES

(1) Carlmark, A.; Malmstrom, E. E. ATRP Grafting from Cellulose Fibers to Create Block-Copolymer Grafts. *Biomacromolecules* **2003**, *4*, 1740−1745.

(2) Semsarilar, M.; Ladmiral, V.; Perrier, S. Synthesis of a Cellulose Supported Chain Transfer Agent and Its Application to RAFT Polymerization. *J. Polym. Sci., Polym. Chem.* **2010**, *48*, 4361−4365.

(3) Sakurada, I.; Nukushina, Y.; Ito, T. Experimental Determination of the Elastic Modulus of Crystalline Regions in Oriented Polymers. *J. Polym. Sci.* **1962**, *57*, 651−660.

(4) Eichhorn, S. J.; Dufresne, A.; Aranguren, M.; Marcovich, N. E.; Capadona, J. R.; Rowan, S. J.; Weder, C.; Thielemans, W.; Roman, M.; Renneckar, S.; Gindl, W.; Veigel, S.; Keckes, J.; Yano, H.; Abe, K.; Nogi, M.; Nakagaito, A. N.; Mangalam, A.; Simonsen, J.; Benight, A. S.; Bismarck, A.; Berglund, L. A.; Peijs, T. Review: Current International Research into Cellulose Nanofibres and Nanocomposites. *J. Mater. Sci.* **2010**, *45*, 1−33.

(5) Habibi, Y.; Goffin, A. L.; Schiltz, N.; Duquesne, E.; Dubois, P.; Dufresne, A. Bionanocomposites Based on Poly(Epsilon-Caprolactone)-Grafted Cellulose Nanocrystals by Ring-Opening Polymerization. *J. Mater. Chem.* **2008**, *18*, 5002−5010.

(6) Nyström, G.; Mihranyan, A.; Razaq, A.; Lindström, T.; Nyholm, L.; Strømme, M. A Nanocellulose Polypyrrole Composite Based on Microfibrillated Cellulose from Wood. *J. Phys. Chem. B* **2010**, *114*, 4178−4182.

(7) Kang, Y. J.; Chun, S.-J.; Lee, S.-S.; Kim, B.-Y.; Kim, J. H.; Chung, H.; Lee, S.-Y.; Kim, W. All-Solid-State Flexible Supercapacitors Fabricated with Bacterial Nanocellulose Papers, Carbon Nanotubes, and Triblock-Copolymer Ion Gels. *ACS Nano* **2012**, *6*, 6400−6406.

(8) Klemm, D.; Kramer, F.; Moritz, S.; Lindström, T.; Ankerfors, M.; Gray, D.; Dorris, A. Nanocelluloses: A New Family of Nature-Based Materials. *Angew. Chem., Int. Ed.* **2011**, *50*, 5438−5466.

(9) Dong, X. M.; Kimura, T.; Revol, J.-F.; Gray, D. G. Effects of Ionic Strength on the Isotropic−Chiral Nematic Phase Transition of Suspensions of Cellulose Crystallites. *Langmuir* **1996**, *12*, 2076−2082.

(10) Lagerwall, J. P. F.; Schutz, C.; Salajkova, M.; Noh, J.; Hyun Park, J.; Scalia, G.; Bergstrom, L. Cellulose Nanocrystal-Based Materials:

From Liquid Crystal Self-Assembly and Glass Formation to Multifunctional Thin Films. *NPG Asia Mater.* **2014**, *6*, e80.
(11) Pendergraph, S. A.; Klein, G.; Johansson, M. K. G.; Carlmark, A. Mild and Rapid Surface Initiated Ring-Opening Polymerisation of Trimethylene Carbonate from Cellulose. *RSC Adv.* **2014**, *4*, 20737−20743.
(12) Roy, D.; Guthrie, J. T.; Perrier, S. Graft polymerization: Grafting Poly(styrene) from Cellulose via Reversible Addition-Fragmentation Chain Transfer (RAFT) Polymerization. *Macromolecules* **2005**, *38*, 10363−10372.
(13) Marais, A.; Utsel, S.; Gustafsson, E.; Wågberg, L. Towards a Super-Strainable Paper Using the Layer-by-Layer Technique. *Carbohyd. Polym.* **2014**, *100*, 218−224.
(14) Wågberg, L.; Decher, G.; Norgren, M.; Lindström, T.; Ankerfors, M.; Axnäs, K. The Build-Up of Polyelectrolyte Multilayers of Microfibrillated Cellulose and Cationic Polyelectrolytes. *Langmuir* **2008**, *24*, 784−795.
(15) Aulin, C.; Varga, I.; Claesson, P. M.; Wågberg, L.; Lindström, T. Buildup of Polyelectrolyte Multilayers of Polyethyleneimine and Microfibrillated Cellulose Studied by In Situ Dual-Polarization Interferometry and Quartz Crystal Microbalance with Dissipation. *Langmuir* **2008**, *24*, 2509−2518.
(16) Illergard, J.; Enarsson, L. E.; Wagberg, L.; Ek, M. Interactions of Hydrophobically Modified Polyvinylamines: Adsorption Behavior at Charged Surfaces and the Formation of Polyelectrolyte Multilayers with Polyacrylic Acid. *ACS Appl. Mater. Interfaces* **2010**, *2*, 425−433.
(17) Nordgren, N.; Lönnberg, H.; Hult, A.; Malmström, E.; Rutland, M. W. Adhesion Dynamics for Cellulose Nanocomposites. *ACS Appl. Mater. Interfaces* **2009**, *1*, 2098−2103.
(18) Notley, S. M.; Eriksson, M.; Wågberg, L.; Beck, S.; Gray, D. G. Surface Forces Measurements of Spin-Coated Cellulose Thin Films with Different Crystallinity. *Langmuir* **2006**, *22*, 3154−3160.
(19) Gustafsson, E.; Johansson, E.; Wågberg, L.; Pettersson, T. Direct Adhesive Measurements Between Wood Biopolymer Model Surfaces. *Biomacromolecules* **2012**, *13*, 3046−3053.
(20) Eriksson, M.; Notley, S. M.; Wågberg, L. Cellulose Thin Films: Degree of Cellulose Ordering and Its Influence on Adhesion. *Biomacromolecules* **2007**, *8*, 912−919.
(21) Rundlöf, M.; Karlsson, M.; Wågberg, L.; Poptoshev, E.; Rutland, M.; Claesson, P. Application of the JKR Method to the Measurement of Adhesion to Langmuir−Blodgett Cellulose Surfaces. *J. Colloid Interface Sci.* **2000**, *230*, 441−447.
(22) Holmberg, M.; Berg, J.; Stemme, S.; Ödberg, L.; Rasmusson, J.; Claesson, P. Surface Force Studies of Langmuir−Blodgett Cellulose Films. *J. Colloid Interface Sci.* **1997**, *186*, 369−381.
(23) Poptoshev, E.; Rutland, M. W.; Claesson, P. M. Surface Forces in Aqueous Polyvinylamine Solutions. 2. Interactions between Glass and Cellulose. *Langmuir* **1999**, *16*, 1987−1992.
(24) Shull, K. R.; Ahn, D.; Chen, W. L.; Flanigan, C. M.; Crosby, A. J. Axisymmetric Adhesion Tests of Soft Materials. *Macromol. Chem. Phys.* **1998**, *199*, 489−511.
(25) Bartlett, M. D.; Croll, A. B.; King, D. R.; Paret, B. M.; Irschick, D. J.; Crosby, A. J. Looking Beyond Fibrillar Features to Scale Gecko-Like Adhesion. *Adv. Mater.* **2012**, *24*, 1078−1083.
(26) Bartlett, M. D.; Croll, A. B.; Crosby, A. J. Designing Bio-Inspired Adhesives for Shear Loading: From Simple Structures to Complex Patterns. *Adv. Funct. Mater.* **2012**, *22*, 4985−4992.
(27) Edgar, C.; Gray, D. Smooth Model Cellulose I Surfaces from Nanocrystal Suspensions. *Cellulose* **2003**, *10*, 299−306.
(28) Berthold, F.; Gustafsson, K.; Berggren, R.; Sjöholm, E.; Lindström, M. Dissolution of Softwood Kraft Pulps by Direct Derivatization in Lithium Chloride/Dimethylacetamide. *J. Appl. Polym. Sci.* **2004**, *94*, 424−431.
(29) Turbak, A. F.; El-Kafrawy, A.; Snyder, F. W., Jr.; Auerbach, A. B. *Solvent system for cellulose*, U.S. Patent 4,302,252, 1981.
(30) Potthast, A.; Rosenau, T.; Buchner, R.; Röder, T.; Ebner, G.; Bruglachner, H.; Sixta, H.; Kosma, P. The Cellulose Solvent System *N,N*-Dimethylacetamide/Lithium Chloride Revisited: The Effect of Water on Physicochemical Properties and Chemical Stability. *Cellulose* **2002**, *9*, 41−53.
(31) Carrick, C.; Ruda, M.; Pettersson, B.; Larsson, P. T.; Wågberg, L. Hollow Cellulose Capsules from CO_2 Saturated Cellulose Solutions—Their Preparation and Characterization. *RSC Adv.* **2013**, *3*, 2462−2469.
(32) Forsström, J.; Eriksson, M.; Wågberg, L. A New Technique for Evaluating Ink−Cellulose Interactions: Initial Studies of the Influence of Surface Energy and Surface Roughness. *J. Adhes. Sci. Technol.* **2005**, *19*, 783−798.
(33) van Oss, C. J.; Chaudhury, M. K.; Good, R. J. Monopolar Surfaces. *Adv. Colloid Interface Sci.* **1987**, *28*, 35−64.
(34) Van Oss, C. J.; Chaudhury, M. K.; Good, R. J. Interfacial Lifshitz−van der Waals and Polar Interactions in Macroscopic Systems. *Chem. Rev.* **1988**, *88*, 927−941.
(35) Volpe, C. D.; Siboni, S. Some Reflections on Acid−Base Solid Surface Free Energy Theories. *J. Colloid Interface Sci.* **1997**, *195*, 121−136.
(36) Hermans, P. H.; Weidinger, A. X-ray Studies on the Crystallinity of Cellulose. *J. Polym. Sci.* **1949**, *4*, 135−144.
(37) Carrick, C.; Lindström, S. B.; Larsson, P. T.; Wågberg, L. Lightweight, Highly Compressible, Noncrystalline Cellulose Capsules. *Langmuir* **2014**, *30*, 7635−7644.
(38) Owen Michael, J.: Siloxane Surface Activity. In *Silicon-Based Polymer Science*; American Chemical Society: Washington, DC, 1989; Vol. *224*, pp 705−739.
(39) Enders, S.; Kahl, H.; Winkelmann, J. Surface Tension of the Ternary System Water + Acetone + Toluene. *J. Chem. Eng. Data* **2007**, *52*, 1072−1079.
(40) Stiernstedt, J.; Nordgren, N.; Wågberg, L.; Brumer Iii, H.; Gray, D. G.; Rutland, M. W. Friction and Forces between Cellulose Model Surfaces: A Comparison. *J. Colloid Interface Sci.* **2006**, *303*, 117−123.
(41) Notley, S. M.; Pettersson, B.; Wagberg, L. Direct Measurement of Attractive van der Waals' Forces Between Regenerated Cellulose Surfaces in an Aqueous Environment. *J. Am. Chem. Soc.* **2004**, *126*, 13930−13931.
(42) Shull, K. R. Contact Mechanics and the Adhesion of Soft Solids. *Mater. Sci. Eng., R* **2002**, *36*, 1−45.
(43) Bartlett, M. D.; Crosby, A. J. Scaling Normal Adhesion Force Capacity with a Generalized Parameter. *Langmuir* **2013**, *29*, 11022−11027.
(44) Pendergraph, S. A.; Park, J. Y.; Hendricks, N. R.; Crosby, A. J.; Carter, K. R. Facile Colloidal Lithography on Rough and Non-planar Surfaces for Asymmetric Patterning. *Small* **2013**, *9*, 3037−3042.
(45) Pendergraph, S. A.; Bartlett, M. D.; Carter, K. R.; Crosby, A. J. Enhancing Adhesion of Elastomeric Composites through Facile Patterning of Surface Discontinuities. *ACS Appl. Mater. Interfaces* **2014**, *6*, 6845−6850.
(46) Davis, C. S.; Martina, D.; Creton, C.; Lindner, A.; Crosby, A. J. Enhanced Adhesion of Elastic Materials to Small-Scale Wrinkles. *Langmuir* **2012**, *28*, 14899−14908.
(47) Chaudhury, M. K.; Whitesides, G. M. Direct Measurement of Interfacial Interactions Between Semispherical Lenses and Flat Sheets of Poly(dimethylsiloxane) and Their Chemical Derivatives. *Langmuir* **1991**, *7*, 1013−1025.
(48) Schneider, F.; Draheim, J.; Kamberger, R.; Wallrabe, U. Process and Material Properties of Polydimethylsiloxane (PDMS) for Optical MEMS. *Sens. Actuators, A* **2009**, *151*, 95−99.
(49) Chaudhury, M. K. Surface Free Energies of Alkylsiloxane Monolayers Supported on Elastomeric Polydimethylsiloxanes. *J. Adhes. Sci. Technol.* **1993**, *7*, 669−675.
(50) Fritz, J. L.; Owen, M. J. Hydrophobic Recovery of Plasma-Treated Polydimethylsiloxane. *J. Adhes.* **1995**, *54*, 33−45.
(51) Kim, J.; Chaudhury, M. K.; Owen, M. J. Hydrophobic Recovery of Polydimethylsiloxane Elastomer Exposed to Partial Electrical Discharge. *J. Colloid Interface Sci.* **2000**, *226*, 231−236.